Proceedings of the 9ICEG
9th International Congress on Environmental Geotechnics
25-28 June, 2023 | Chania, Greece

https://doi.org/10.53243/ICEG2023-165

Hydraulic conductivity of geopolymer-bentonite cutoff wall backfill for contamination control

Qin-Pei Xue[1], Hong-Xin Chen[2,*], Shi-Jin Feng[3], Qi-Teng Zheng[4]

[1]PhD Candidate, Tongji University, Shanghai, China, email: 2111340@tongji.edu.cn

[2]Associate Professor, Tongji University, Shanghai, China, email: chenhongxin@tongji.edu.cn

[3]Professor, Tongji University, Shanghai, China, email: fsjgly@tongji.edu.cn

[4]Assistant Professor, Tongji University, Shanghai, China, email: 08qitengzheng@tongji.edu.cn

ABSTRACT

Cutoff wall is one of the most effective technologies for the soil and groundwater contamination control. However, conventional backfill consisting of ordinary portland cement (OPC) inevitably deteriorate under mechanical, chemical, and environmental stresses. The damage of cut-off walls can undermine their mechanical properties and durability, impacting their serviceability and reliability. This paper proposed an innovative geopolymer cutoff wall backfill (GCWB) that is composed of fly ash (FA), sodium silicate (Na_2SiO_3) and sand. On this basis, bentonite with different content was further added to improve the durability, thus forming geopolymer-bentonite cutoff wall backfill (GBCWB). The hydraulic conductivity of GBCWB were tested, then the optimal material ratio was determined. In order to evaluate the durability of GBCWB in dry-wet cycle test, the microstructural characteristics were assessed by Scanning Electron Microscopy (SEM) with Energy Dispersive Spectroscopy (EDS). The overall performance proved that GBCWB is promising to be used in contamination control.

Keywords: Geopolymer, Bentonite, Cutoff wall, Hydraulic conductivity, Dry-wet cycle, Durability

1 INTRODUCTION

Vertical cutoff wall is one of the most effective technologies to restrict the migration of contaminants (Britton et al., 2004; Chen et al., 2019; Peng et al., 2021), which has been widely employed in plenty of contaminated sites (Ata et al., 2015; Du et al., 2015; Takai et al., 2016; Peng et al., 2020; Zhan et al., 2022). European and American countries possess an abundance of high-quality sodium-based bentonite resources, thus making it a widespread choice for cutoff walls (Opdyke & Evans, 2005; Evans et al., 2021; Ji et al., 2021). However, due to the scarcity of such resources in China, traditional waterproof curtains such as underground continuous walls made of cement-based materials, cement-soil mixing piles, and plastic concrete are mainly employed as pollution-prevention isolation walls, which are highly energy-intensive, carbon-intensive, expensive, and have poor chemical compatibility. The barrier performance often fails to meet the requirements of pollution control (Ryan & Day, 2005).

Consequently, the improvement of isolation wall materials has been widely studied. Currently, industrial solid wastes (ISW) such as granulated blast furnace slag (GGBS) and fly ash, which are abundant and cost-effective, have gradually been applied to cutoff wall backfills to partially replace cement (Opdyke & Evans, 2005; Ji et al., 2021; Jefferis, 1997; Talefirouz et al., 2016). Jefferis (1997) reported that increasing slag content to above 60% in the cement-bentonite (CB) wall reduces the hydraulic conductivity to below 1×10^{-9} m/s after three months curing. Opdyke & Evans (2005) conducted permeability tests on twenty-one different mixtures of slag-CB backfills, and found that 0 to 60% slag replacement has little effect on hydraulic conductivity of the slag-CB mixtures, but the hydraulic conductivity drastically decreases to 2×10^{-10} m/s as the slag replacement increases from 70 to 80%. Talefirouz & Omer (2016) also discovered that the hydraulic conductivity is below 1×10^{-9} m/s for the slag replacement of 50% and 90 days of curing period. Therefore, partially replacing OPC by adding ISW can improve the performance of cement-based cutoff wall to a certain extent.

Geopolymers is a novel green cementitious material with a three-dimensional networked key-joint structure, which is significantly different from traditional anti-pollution barrier materials in terms of strength, permeability, durability (Arulrajah, 2016; Kua, 2016; Liu & Chen, 2016; Wang et al., 2021). In China, a colossal amount of industrial solid waste is produced each year, most of which are inorganic silicate and aluminate minerals that can theoretically form geopolymers under the action of appropriate activators. It can effectively reduce energy consumption, carbon consumption, and pollutant emissions, as well as resolving the issue of massive solid waste storage and environmental pollution. At present, numerous scholars have conducted extensive research on the strength characteristics of geopolymers, but the research on the permeability and durability of geopolymer applied to polluted sites as cutoff wall backfill is still relatively limited. Recently, some studies have been carried out to completely replace OPC by geopolymer in preparing cutoff wall backfill (Huang et al., 2021; Wu et al., 2019a, 2021b). Huang et al. (2021) prepared a new cutoff wall backfill with reactive magnesium oxide, GGBS, bentonite, and water. Through microscopic tests, the generated hydration products effectively fill the matrix pores to form a dense microstructure, making its mechanical and hydraulic properties better than those of ordinary slag-CB barrier, in which the minimum hydraulic conductivity is close to 1×10^{-10} m/s. Wu et al. (2019a, 2021b) also proposed an innovative cutoff wall backfill consisting of reactive magnesium oxide, GGBS, bentonite, clayey sand, and water, its hydraulic conductivity in water and contaminant solution is between 1.1×10^{-10} and 6.3×10^{-10} m/s after a curing age of 90 days, and the unconfined compressive strength is larger than 100 kPa.

As abovementioned, geopolymer is a promising material to prepare cutoff wall backfill, which can completely substitute OPC. Furthermore, the dry-wet cycles may occur due to precipitation, drought, and ground water fluctuation, which change the water content and internal microstructure of cutoff wall and significantly influence its barrier performance. However, relative experimental study is quite limited, especially for geopolymer cutoff wall. Therefore, a geopolymer-bentonite cutoff wall backfill (GBCWB) was proposed in this study, which consists of reactive sodium silicate, fly ash, bentonite, sand, and water. This study will provide a better understanding of the barrier performance of geopolymer and is helpful for contamination control.

2 MATERIALS AND TESTING PROGRAM

2.1 Materials

In this study, sand, fly ash, sodium silicate, bentonite and tap water were used to generate cutoff wall backfill. The fine-grained sand used in this study is from Fujian, China. The standard sand was dried and sieved in the laboratory. The raw material used for preparing geopolymer in this study is a grey powdered fly ash (FA) produced by Zhanteng Mining Company in China. The main components were SiO_2 and Al_2O_3, accounting for more than 82% of the total weight. The detailed chemical compositions of the FA are shown in Table 1. In this study, sodium silicate (Na_2SiO_3) with modulus of 1, 1.2 and 1.4 was used as the alkali-activator for geopolymerization, which was a pure chemically powder produced by Borun Material Company in Henan, China. The natural sodium bentonite used in this study were provided by Zhengzhou Zhenghou Trading Co. LTD (Henan, China). Sodium bentonite was used to further improve the performance of cutoff wall backfill, with swell index and specific surface area being 24.5 mL/2 g, 586.1 m^2/g, respectively.

Table 1. *Chemical compositions of fly ash.*

Composition	SiO_2	Al_2O_3	CaO	Fe_2O_3	TiO_2	K_2O	SO_3	MgO
Percentage (%)	48.85	33.97	5.51	5.33	2.1	1.07	0.92	0.55

2.2 Testing program

The primary purpose of this study was to determine the optimal material ratio of GBCWB and explore its durability during dry-wet cycles. Hence, the testing scheme was divided into two steps. The first step focused on the optimal material ratio of GBCWB, including the content of fly ash, the modulus of sodium silicate, the content of sodium silicate and the content of bentonite. The second step focused on evaluation of the durability of GBCWB during dry-wet cycles.

(1) Tests to determine the optimum material ratio of GBCWB
In order to reduce the test number, orthogonal test scheme was adopted, including three-factors and three-levels, as shown in Tables 2 and 3. For example, 30FA1.2M12S represents that the fly ash weight

was 30% of the test sand weight, the modulus of sodium silicate was 1.2, and sodium silicate weight was 12% of the fly ash weight. In this study, cylindrical samples with a diameter of 61.87 mm and a height of 40 mm were prepared at 7d, 14d and 28d curing ages, respectively. Variable head permeability test was carried out using rigid wall permeameter according to ASTM D5084 (2016). Hydraulic conductivity is the most important index to evaluate the barrier performance of cutoff wall. Hence, permeability test was conducted to determine the optimal material ratio with the lowest hydraulic conductivity. On the basis of the optimal ratio of GCWB, bentonite with different content was further added to improve the durability, as shown in Table 4.

Table 2. *Three-factors and three-levels orthogonal table.*

Level \ Factor	A (Fly ash content)	B (Modulus of Na_2SiO_3)	C （Content of Na_2SiO_3）
1	20%	1	10%
2	30%	1.2	12%
3	40%	1.4	14%

Table 3. *Orthogonal experiment scheme.*

No.	Fly ash (%)	Modulus	Alkali-activator (%)
20FA1M14S	20	1	14
20FA1.2M10S	20	1.2	10
20FA1.4M12S	20	1.4	12
30FA1M10S	30	1	10
30FA1.2M12S	30	1.2	12
30FA1.4M14S	30	1.4	14
40FA1M12S	40	1	12
40FA1.2M14S	40	1.2	14
40FA1.4M10S	40	1.4	10

Table 4. *Experiment scheme for the optimum mixing ratio of bentonite in GBCWB*

No.	GBCWB1	GBCWB2	GBCWB3
Mixing ratio of bentonite (%)	3	6	9

(2) Tests to evaluate the durability of GBCWB during dry-wet cycles
Dry-wet cycle test was conducted to evaluate the durability of GBCWB. The material ratios with the lowest hydraulic conductivity were adopted for the dry-wet cycle test, respectively. The samples had the same size as that in the permeability test and were cured for 28 days. A total of ten dry-wet cycles were considered according to ASTM D4843-88 (2016). Two types of wet cycle environment were considered here, including water and contaminant solution ($CaCl_2$ with a concentration of 50 mmol/L). After each dry-wet cycle, the hydraulic conductivity was tested.

Microstructural analysis was carried to study the change in microscale features. After low-temperature drying, the GBCWB before and after the dry-wet cycle(s) were cut into 5 × 5 × 5 mm samples, which were carefully polished and leveled. The microstructure observations were conducted by JSM-5900 Scanning Electron Microscope (SEM) at different magnification times. The energy dispersive spectrometer (EDS) tests were also conducted to further reveal the barrier mechanism of the GBCWB in water and contaminant solutions.

2.3 Sample preparation

According to the ratio design proposed in the experimental program, each group of test sand, fly ash, sodium silicate and bentonite weighed respectively, and the weighing error shall not exceed ± 1% of the design value. Firstly, the sand, fly ash (and bentonite) were fully dry mixed, then the sodium silicate was fully stirred until dissolved with the water (60 °C), and finally the mixture of sand, fly ash (and bentonite) was fully mixed with the sodium silicate solution. Lubricant oil was evenly daubed to specimen preparation mold's inner surface before filling the sample to ensure the specimen's integrity during mold removal. The well-mixed cutoff wall backfill was filled into the mold in layers and fully vibrated at the same time to discharge excess bubbles. When the specimen preparation was completed, all specimens were numbered and left in the constant temperature and humidity curing box for curing (the curing temperature was 19-21 °C and the humidity was about 96%), as shown in Figure 1.

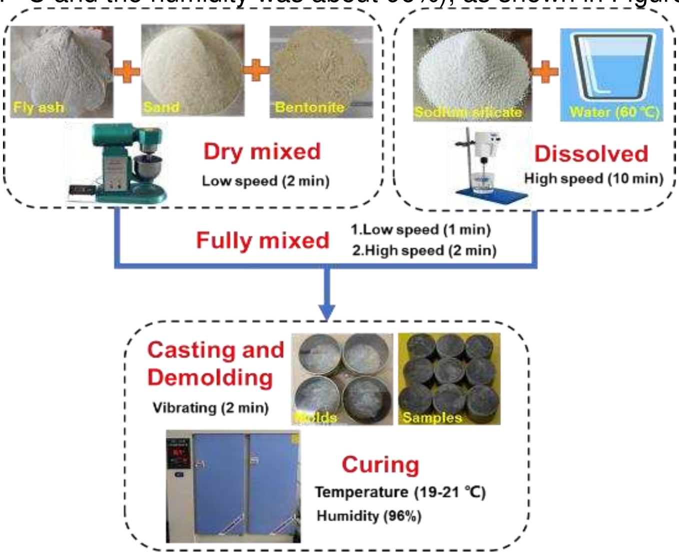

Figure 1. *Sample preparation procedures.*

3 HYDRAULIC CONDUCTIVITY OF THE GBCWB

3.1 Hydraulic conductivity of GCWB

The test results of GCWB using water as the permeant liquid after different curing ages are shown in Figure 2. It can be observed that the hydraulic conductivity of GCWB decreased with the increase of curing age. The reason is that, after the alkali-activator is added to the fly ash, geopolymer is generated through geopolymerization reaction, and as the reaction progresses, the generated gel fills the sand particles, making the sample dense, thus resulting in the decrease of hydraulic conductivity. The hydraulic conductivity of GCWB cured for 14 and 28 days all met the design requirement of cement-based cutoff wall (< 1×10^{-8} m/s), and only the 20FA1M14S and 20FA1.4M12S samples cured for 7 days cannot meet the requirement (Wu et al., 2019a, 2021b). Moreover, from a holistic perspective, the decrease in hydraulic conductivity for different ratios of backfill within the curing period of 7 to 14 days was far greater than that of 14 to 28 days. The reason is that the dissolution of fly ash starts from the surface, with the initial reaction being relatively rapid, after a large amount of gel is generated, it covers the undissolved fly ash surface, hindering the dissolution reaction from continuing. This leads to the synthesis of geopolymer becoming slower with the prolongation of curing time, and the geopolymerization reaction tends to be stable. Consequently, the hydraulic conductivity of the sample decreased at a smaller rate in the later stage.

In the orthogonal experiment design method, range analysis is conducted on the obtained experimental index results. According to the variation of the experimental index with the levels of each factor, the optimal level of each factor can be analysed. In addition, the importance ranking of the factors affecting the index can also be obtained, that is, the degree of influence of each factor on the experimental results. Therefore, the hydraulic conductivity was converted into one score through the function ($y = -\log_{10}k_w$, where k_w is the hydraulic conductivity in water), and the range analysis of the score was carried out. In Table 5, Ki (i = 1, 2, 3 is the level number) is the sum of the hydraulic conductivity values corresponding to level i for a single factor. For example, $K1$ of factor A represents the sum of hydraulic conductivity conversion values y of the three samples with fly ash content of 20%, as shown in Table 5. ki is the average value, i.e. $ki = Ki / 3$. For example, $k1$ of factor A represents the average hydraulic conductivity of the three samples with fly ash content of 20%. R is the range of Ki, namely, the difference between the maximum value and the minimum value of Ki. The larger the value of R under a single factor is, the greater the influence of this factor on the hydraulic conductivity will be. According to the value of R, the relative importance of the influence factors can be determined.

Based on the range analysis, it can be concluded that the optimal material ratio with the lowest hydraulic conductivity can be obtained as A3B2C2, that is 40FA1.2M12S. This combination was not included in the orthogonal experiment scheme (see Table 3), so additional tests were conducted for this combination. The hydraulic conductivity can be as low as 4.83 × 10^{-11} m/s at 28d curing age, which is smaller than the lowest value of the orthogonal test results (6.71 × 10^{-11} m/s for 30FA1.2M12S at 28d curing age). This further confirms that the orthogonal test and analysis method is reliable.

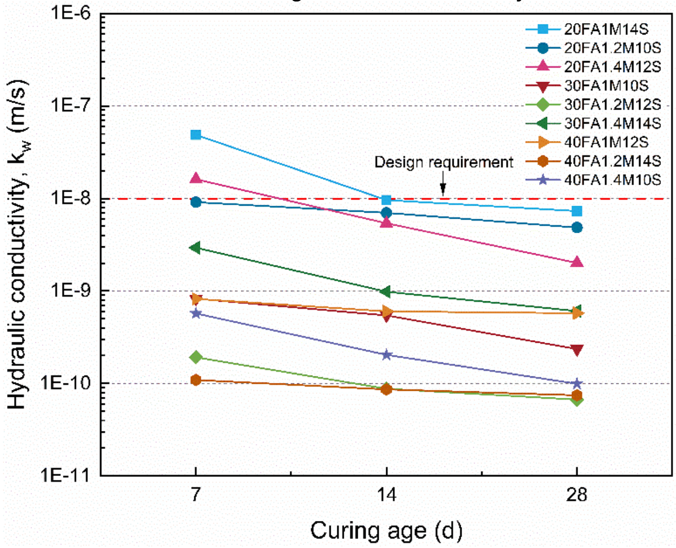

Figure 2. *Hydraulic conductivity of GCWB at different curing ages.*

Table 5. *Range analysis of hydraulic conductivity.*

Curing age		**A**	**B**	**C**
7d	*K*1	23.15	25.48	26.37
	*K*2	27.33	27.72	26.60
	*K*3	28.29	25.57	25.81
	*k*1	7.72	8.49	8.79
	*k*2	9.11	9.24	8.87
	*k*3	9.43	8.52	8.60
	R	5.14	2.24	0.79
	Ranking		A>B>C	
	Optimal ratio		A3B2C2	
14d	*K*1	24.44	26.50	27.11
	*K*2	28.33	28.27	27.55
	*K*3	28.96	26.97	27.08
	*k*1	8.15	8.83	9.04
	*k*2	9.44	9.42	9.18
	*k*3	9.65	8.99	9.03
	R	4.52	1.76	0.46
	Ranking		A>B>C	
	Optimal ratio		A3B2C2	
28d	*K*1	25.15	27.00	27.94
	*K*2	29.02	28.61	28.11
	*K*3	29.37	27.92	27.48
	*k*1	8.38	9.00	9.31
	*k*2	9.67	9.54	9.37
	*k*3	9.79	9.31	9.16
	R	4.22	1.61	0.63
	Ranking		A>B>C	
	Optimal ratio		A3B2C2	

3.2 Hydraulic conductivity of GBCWB

The test results of GBCWB and GCWB with the lowest hydraulic conductivity (40FA1.2M12S) after different curing ages are shown in Figure 3. The results show that the hydraulic conductivity of GBCWB decreased with the increase of curing age. The hydraulic conductivity of GBCWB all met the design requirements of cutoff wall (<1 × 10^{-8} m/s). In particular, the average hydraulic conductivity of GBCWB1 (4.73 × 10^{-11} m/s) was slightly lower than that of 40FA1.2M12S at 28d curing age. With the increase of bentonite content, the hydraulic conductivity of GBCWB increased. With the increase of bentonite content, due to the expansive nature of bentonite itself, it can fill the pores in the matrix and reduce the flowing path. However, when the amount of bentonite is excessive, the bentonite needs to absorb more water, which seriously affects the hydration of geopolymer. It increases the internal pores of matrix, thus increasing the hydraulic conductivity of GBCWB. Therefore, the amount of bentonite in the backfill should be controlled over a reasonable range. In this study, 3% bentonite was the best proportion, that is GBCWB1.

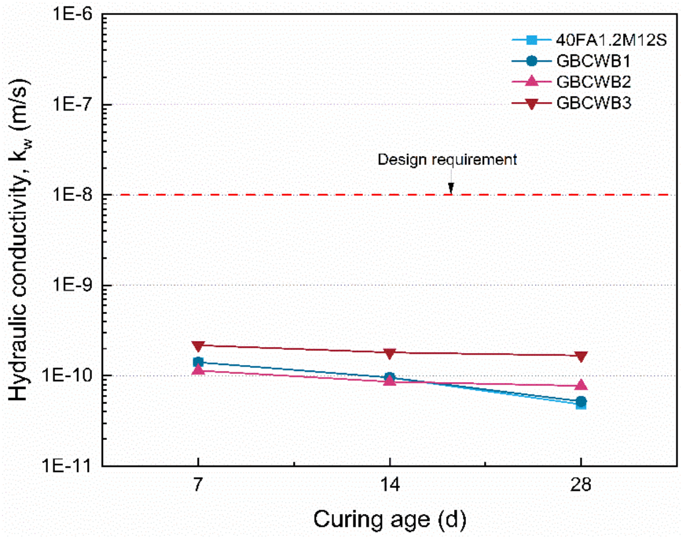

Figure 3. *Hydraulic conductivity of GBCWB at different curing ages.*

4 DURABILITY OF THE GBCWB UNDER DRY-WET CYCLES

4.1 Variation of hydraulic conductivity with the increase of dry-wet cycles

The samples with the lowest hydraulic conductivity (40FA1.2M12S and GBCWB1) after 28d curing age were adopted for further studying the durability of GBCWB. In the dry-wet cycle test, the water and contaminant solution were used for soaking the samples, and the variation of hydraulic conductivity with the increase of cycles is shown in Figure 4. It can be found that the hydraulic conductivity of GCWB increased sharply by two orders of magnitude after the 1st dry-wet cycle in water, indicating that the stress caused by dry shrinkage and wet expansion changed the internal microstructure of the GCWB. The subsequent dry-wet cycles had little effect on the hydraulic conductivity, which changed little and was slightly larger than 1×10^{-8} m/s, revealing that the internal microstructure of the GCWB had been stable. On the contrary, the hydraulic conductivity of GBCWB gradually increased with the dry-wet cycles. Until the 7th cycle, the hydraulic conductivity was slightly higher than 1×10^{-8} m/s. The durability of GBCWB in water was much better than that of GCWB.

Compared with test results in water, the variation of hydraulic conductivity in $CaCl_2$ solution was overall the same, indicating that the influence of contaminant on the durability was weak. In particular, the hydraulic conductivity of GBCWB reached 1×10^{-8} m/s after the 5th cycle and tended to be stable similar to that of GCWB. It shows that the durability of GBCWB in $CaCl_2$ solution was also better than that of GCWB. It is interesting that k_c can be slightly smaller than k_w after hydraulic conductivity became stable. The possible reason is that the aluminosilicate gel generated by the geopolymer solidifies the metal ions in the contaminant solution through adsorption and cementation. Further explanation will be provided in the later microscopic analysis.

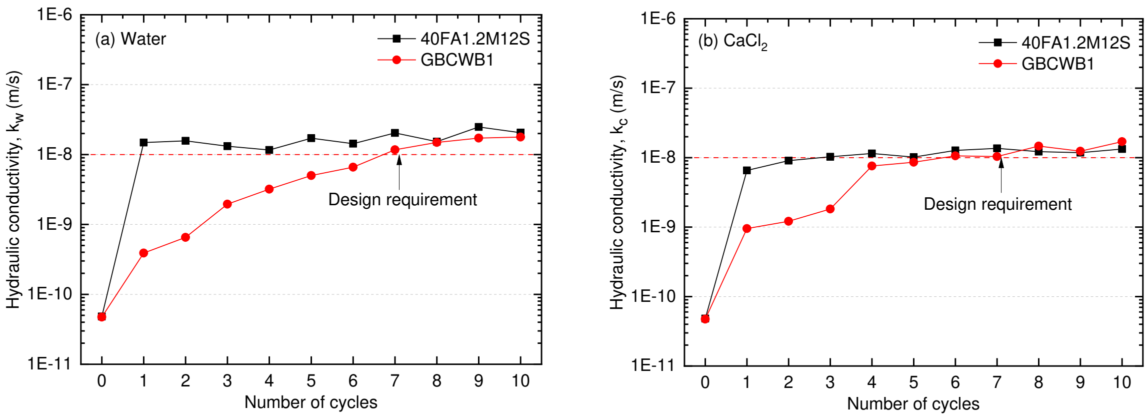

Figure 4. *Variation of hydraulic conductivity with the increase of dry-wet cycles: (a) in water; (b) in $CaCl_2$ solution.*

4.2 Microstructural analysis

To further evaluate the durability of GBCWB, microstructure observations were carried out via scanning electron microscopy (SEM) at a magnification of 1000 after the 10th dry-wet cycle in water and contaminant solution, respectively. Figure 5a shows the microstructures of GCWB after the 10th dry-wet cycle in water. It is obvious that there were some cracks in the samples. It is noteworthy that unoriented gels were wrapped with mineral crystals and bridged on both sides of the fracture, which can effectively block the expansion of cracks. Numerous large aggregates were generated inside the GCWB wrapped or cemented by unoriented gels. Figure 5b shows the microstructures of GCWB after the 10th dry-wet cycle in the 50 mmol/L $CaCl_2$ solution. There were also cracks in the sample, but the structure inside the matrix was relatively tight compared with that in water. In addition, the spherical fly ash particles that did not participate in the geopolymerization were also exposed at the fracture surface of the crack.

Figure 5c-d illustrates the microstructures of GBCWB after the 10th dry-wet cycle in water and 50 mmol/L $CaCl_2$ solution, respectively. It indicates that a large number of fibrous hydration products with stable crystallinity still existed in the GBCWB matrix after the 10th dry-wet cycle. In addition, it can be found that the cracks were significantly reduced compared with GCWB. The micropores were effectively filled by gel and the compactness increased. Expansibility is the principal feature of bentonite, so it also filled the micro-pores of the sample, which gradually reduced the micro-pores of the sample. It significantly delayed the generation and development of cracks in the matrix.

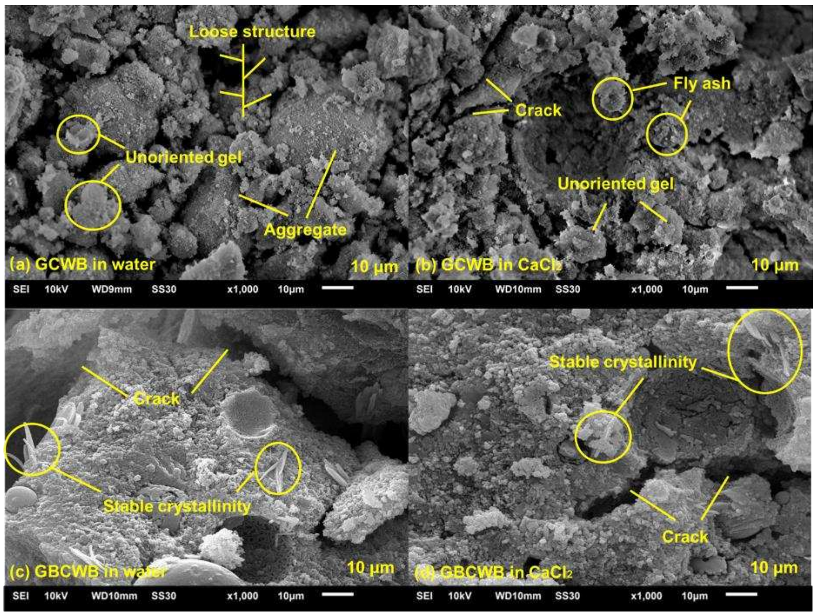

Figure 5. *Microstructures after the 10th dry-wet cycle: (a) GCWB in water, (b) GCWB in $CaCl_2$; (a) GBCWB in water, (b) GBCWB in $CaCl_2$.*

To sum up, the GBCWB had better resistance than GCWB under dry-wet cycles in both water and the contaminant solution, which can effectively resist the stress caused by dry shrinkage and wet expansion and block the erosion of contaminants.

5 CONCLUSIONS

A geopolymer-bentonite cutoff wall backfill (GBCWB) consisting of reactive sodium silicate, fly ash, bentonite, sand, and water was proposed in this study. Through macroscopic and microscopic tests, the hydraulic conductivity and durability were investigated. The GBCWB performed better than GCWB under the dry-wet cycles in water and contaminant solution ($CaCl_2$), indicating that it is a promising antifouling cutoff wall material. Some major conclusions are highlighted as follows:

(1) According to the orthogonal analysis, the optimal material ratios of GCWB and GBCWB with the lowest hydraulic conductivity were 40FA1.2M12S and GBCWB1 (3% bentonite). The hydraulic conductivity of GCWB and GBCWB can achieve 4.83×10^{-11} m/s and 4.73×10^{-11} m/s after cured for 28 days, respectively.

(2) Under the effect of dry-wet cycles, the hydraulic conductivity of GCWB increased sharply by two orders of magnitude after the 1st dry-wet cycle and tended to be stable in the subsequent dry-wet cycles (slightly larger than 1×10^{-8} m/s). The hydraulic conductivity of GBCWB in water and contaminant solution gradually increased with the dry-wet cycle, and was slightly higher than 1×10^{-8} m/s until the fifth and seventh cycles, respectively.

(3) According to the analysis of microstructure, the cracks in GBCWB were significantly reduced compared with GCWB after the dry-wet cycles. The expansion characteristics of bentonite and the generation of gel can effectively fill the micro-pores and make the sample more compact. The GBCWB had better resistance than GCWB under dry-wet cycles in both water and the contaminant solution, which can effectively resist the stress caused by dry shrinkage and wet expansion and block the erosion of contaminants.

6 ACKNOWLEDGEMENTS

Much of the work described in this paper was supported by the National Key Research and Development Program of China under Grant No. 2020YFC1808103, the National Natural Science Foundation of China under Grant Nos. 42077250 and 42277148, the Shanghai Rising-Star Program under Grant No. 22QA1409700, the Top Discipline Plan of Shanghai Universities-Class I, and the Fundamental Research Funds for the Central Universities. The authors would like to greatly acknowledge all these financial supports and express their most sincere gratitude.

REFERENCES

Arulrajah A., Mohammadinia A., Phummiphan I., Horpibulsuk S., Samingthong W. (2016). Stabilization of recycled demolition aggregates by geopolymers comprising calcium carbide residue, fly ash and slag precursors. Construction and Building Materials, 114, 864-873.

ASTM D4843-88. (2016). Standard Test Method for Wetting and Drying Test of Solid Wastes, West Conshohocken, PA.

ASTM D5084. (2016). Standard Test Methods for Measurement of Hydraulic Conductivity of Saturated Porous Materials Using a Flexible Wall Permeameter, West Conshohocken, PA.

Ata A.A., Salem T.N., Elkhawas N.M. (2015). Properties of soil-bentonite-cement bypass mixture for cutoff walls. Construction and Building Materials, 93, 950-956.

Britton J.P., Filz G.M., Herring W.E. (2004). Measuring the hydraulic conductivity of soil-bentonite backfill. Journal of Geotechnical and Geoenvironmental Engineering,130 (12), 1250-1258.

Chen Z.L., Feng S.J., Chen H.X., Peng M.Q., Li Y.C., Zhu Z.W. (2019). Analytical solution for transport of degradable contaminant in cut-off wall and aquifer. Environmental Geotechnics 1-13.

Du Y.J., Fan R.D., Reddy K.R., Liu S.Y., Yang Y.L. (2015). Impacts of presence of lead contamination in clayey soil–calcium bentonite cutoff wall backfills. Applied Clay Science, 108, 111-122.

Evans J.C., Larrahondo J.M., Yeboah N.N.N. (2021). Fate of bentonite in slag-cement-bentonite slurry trench cut-off walls for polluted sites. Environmental Geotechnics, 40, 1-13.

Huang X., Li J.S., Guo M.Z., Xue Q., Du Y.J., Wan Y., Liu L., Poon C.S. (2021). Using MgO activated slag and calcium bentonite slurry to produce a novel vertical barrier material: Performances and mechanisms. Construction and Building Materials, 291, 123365.

Jefferis S.A. (1997). The origins of the slurry trench cut-off and a review of cement-bentonite cut-off walls in the UK.

Ji X., Ye C., Zhou J., He K., Zhu R., Xiang H., Liu J., Xie Z., Liao B. (2021). Study on the microscale structure and barrier mechanism of magnesium phosphate cement modified with fly ash cutoff walls for lead pollution in groundwater. Construction and Building Materials, 308, 124994.

Kua T.A., Arulrajah A., Horpibulsuk S., Du D.Y., Shen S.L. (2016). Strength assessment of spent coffee grounds-geopolymer cement utilizing slag and fly ash precursors. Construction and Building Materials, 115, 565-575.

Liu N., Chen B. (2016). Experimental research on magnesium phosphate cements containing alumina. Construction and Building Materials, 121, 354-360.

Opdyke S.M., Evans J.C. (2005). Slag-cement-bentonite slurry walls. Journal of Geotechnical and Geoenvironmental Engineering, 131 (6), 673-681.

Peng C.H., Feng S.J., Zheng Q.T., Ding X.H., Chen Z.L., Chen H.X. (2020). A two-dimensional analytical solution for organic contaminant diffusion through a composite geomembrane cut-off wall and an aquifer. Computers and Geotechnics, 119, 103361.

Peng C.H., Feng S.J., Chen H.X., Ding X.H. (2021). An analytical model for one-dimensional diffusion of degradable contaminant through a composite geomembrane cut-off wall. Journal of Contaminant Hydrology, 242, 103845.

Ryan C.R., Day S.R. (2002). Soil-cement-bentonite slurry walls. Geotechnical Special Publication, 1, 713-727.

Takai A., Inui T., Katsumi T. (2016). Evaluating the hydraulic barrier performance of soil-bentonite cutoff walls using the piezocone penetration test. Soils and Foundations, 56 (2), 277-290.

Talefirouz D., Çokça E., Omer J. (2016). Use of granulated blast furnace slag and lime in cement-bentonite slurry wall construction. International Journal of Geotechnical Engineering, 10 (1), 81-85.

Wang S.N., Xue Q.P., Zhu Y., Li G., Wu Z.J., Zhao K. (2021). Experimental study on material ratio and strength performance of geopolymer-improved soil. Construction and Building Materials, 267, 120469.

Wu H.L., Jin F., Ni J., Du Y.J. (2019). Engineering properties of vertical cutoff walls consisting of reactive magnesia-activated slag and bentonite: workability, strength and hydraulic conductivity. Journal of Materials in Civil Engineering, 31 (11), 04019263.

Wu H.L., Jin F., Zhou A.N., Du Y.J. (2021). The engineering properties and reaction mechanism of MgO-activated slag cement-clayey sand-bentonite (MSB) cutoff wall backfills. Construction and Building Materials, 271, 121890.

Zhan L.T., You Y.Q., Zhao R., Chen C., Chen Y.M. (2022). Centrifuge modelling of lead retardation in soil-bentonite cut-off walls. International Journal of Physical Modelling in Geotechnics, 1-14.